Resource Allocation for Multi-User Molecular Communication Systems Oriented to The Internet of Medical Things

Xuan Chen, Miaowen Wen, *Senior Member, IEEE*, Chan-Byoung Chae, *Fellow, IEEE*, Lie-Liang Yang, *Fellow, IEEE*, Fei Ji, *Member, IEEE*, and Kostromitin Konstantin Igorevich

***Abstract*—Communication between nano-machines is still an important topic in the construction of the Internet of Bio-Nano Things (IoBNT). Currently, molecular communication (MC) is expected to be a promising technology to realize IoBNT. To effectively serve the IoBNT composed of multiple nano-machine clusters, it is imperative to study multiple-access MC. In this paper, based on the molecular division multiple access technology, we propose a novel multi-user MC system, where information molecules with different diffusion coefficients are first employed. Aiming at the user fairness in the considered system, we investigate the optimization of molecular resource allocation, including the assignment of the types of molecules and the number of molecules of a type. Specifically, three performance metrics are considered, namely, min-max fairness for error probability, max-min fairness for achievable rate, and weighted sum rate maximization. Moreover, we propose two assignment strategies for types of molecules, i.e., best-to-best (BTB) and best-to-worst (BTW). Subsequently, for a two-user scenario, we analytically derive the optimal allocation for the number of molecules when types of molecules are fixed for all users. By contrast, for a three-user scenario, we prove that the BTB and BTW schemes with the optimal allocation for the number of molecules can provide the lower and upper bounds on system performance, respectively. Finally, numerical results show that the combination of BTW and the optimal allocation for the number of molecules yields better performance than the benchmarks.**

***Index Terms*—Molecular communication, multiple access, combinatorial optimization, molecular resource allocation, user fairness, sum rate.**

I. Introduction

SINCE 2020, COVID-19, a pandemic declared by the World Health Organization (WHO), has been terrifying the worldwide human health. Researchers from all areas including Information and Communications Technology (ICT) and the Internet of Things (IoT) [1], [2] are striving for providing the cutting edge solution to curb the catastrophic effects of COVID-19. Among these studies, the Internet of Medical Things (IoMT), an extension and specialization of IoT in the medical industry, has been considered as a promising technology to realize the remote health diagnosis and monitoring in the time of COVID-19, while reducing the risk of infection and the burden on the healthcare systems [3–6]. IoMT is built upon a variety of technologies, including advanced sensors, especially biosensors. Recently, various novel work aimed at the implementation of nanotechnologies, especially biological nano-sensors to help in various disease diagnosis and treatment, forming the Internet of Bio-Nano Things (IoBNT) [7–9]. At this point, IoBNT can be envisioned as a special realization of IoMT in the nanolayer.

In literatures, a series of communication technologies for biological nano-sensors, such as molecular communication (MC), electromagnetic communication, and acoustic communication, was proposed. Unlike the conventional communication methods, MC is a bio-inspired communication paradigm, whose carrier of information is chemical signals. This means MC has the following properties: 1) small size; 2) energy efficiency; and 3) excellent biocompatibility. Owing to the above advantages, MC is considered to have the potential to coordinate larger groups of nanomachines to perform complex tasks in IoBNT [7–9]. On the other hand, as an interdisciplinary communication mode, MC is capable of serving biomedical fields, such as targeted drug delivery [10], [11], disease diagnosis [12], [13], and health monitoring [14–16] Moreover, during the outbreak of COVID-19, MC can also be employed as an effective tool to model the spread of infections and diseases via aerosols [17–20]. In this context, MC can pave the way for the IoMT in the nanolayer.

Despite these advantages, how nano-machines or nano-users share a common MC medium to correctly implement their own functions is still a great challenge for IoBNT. Inspired by wireless communications, some multiple-access technologies have been proposed in MC, which mainly include molecular code division multiple access (MCDMA), molecular time division multiple access (MTDMA), molecular space division multiple access (MSDMA), and molecular division multiple access (MDMA). Analogous to optical CDMA, the authors of [21] first proposed MCDMA to combat the inter-user interference in multi-user MC systems, where each user is assigned a unique binary sequence as their signature code. Subsequently, in [22], a realistic propagation model for M-CDMA systems was built using the experimental apparatus. Moreover, molecule shift keying (MoSK) modulation was introduced in MCDMA [23], [24]. In literatures, MTDMA

Manuscript received December 20, 2020; accepted January 6, 2021. Date of publication xx xx, 2021; date of current version January 10, 2021. This work was supported in part by the National Natural Science Foundation of China under Grant 61871190, in part by the Natural Science Foundation of Guangdong Province under Grant 2018B030306005, in part by the Pearl River Nova Program of Guangzhou under Grant 201806010171, and in part by the Fundamental Research Funds for the Central Universities under Grant 2019SJ02. *(Corresponding author: Fei Ji, Miaowen Wen.)*

X. Chen, M. Wen, and F. Ji are with the School of Electronic and Information Engineering, South China University of Technology, Guangzhou, China (e-mail: eechenxuan@mail.scut.edu.cn, {eemwwen, eefeiji}@scut.edu.cn).

C.-B. Chae is with the School of Integrated Technology, Yonsei University, Seoul, Korea (e-mail: cbchae@yonsei.ac.kr).

L.-L. Yang is with the School of Electronics and Computer Science, University of Southampton, SO17 1BJ, UK (e-mail: lly@ecs.soton.ac.uk.)

K. K. Igorevich is with the Department of Information Security, NRU South Ural State University, Chelyabinsk, Russia (e-mail: kostromitinki@susu.ru).

has also been investigated, where users share the channel by dividing up time among users [25–30]. The authors of [25] considered a group of bio-nanomachines which multiplex their transmission using TDMA to prevent interference among different sources. Motivated by a network of neurons, the authors of [26] and [29] presented an MTDMA-based network transmission scheme. The authors of [28] and [30] studied the related MTDMA optimization. Considering in MC that the channel impulse response is highly sensitive to the transmission distance, MSDMA thereby was proposed, in which users can identify transmitters based on their locations [31], [32]. Moreover, the authors of [33] proposed the MDMA technique, which uses pheromone diversity to perform several simultaneous transmissions, sharing the same medium without interfering with each other. Following this idea, the authors of [34–37] also suggested to use different types of molecules or different receptors and associated molecules for each receiver connection to create orthogonal channels, so as to achieve multiple access among nano-machines. Among the schemes achieving multiple access, MDMA is generally recognized to be the most straightforward one.

The concept of multiple types of molecules has also been widely used in molecular modulation, forming the MoSK modulation [33, 36, 38, 39]. We noticed that in all the scenarios introducing multiple types of molecules for modulation or multiple access, a common diffusion coefficient is always assumed for all molecules. For isomers, this assumption is reasonable [39]. However, for the IoBNT constructed by a group of nano-machines, it may be difficult to have the required and possibly a big number of isomers to serve the network. Furthermore, due to the identical molecular formula, isomers may share very similar chemical or physical properties, leading to low distinguishability in detection. For example, the mass spectrometer involved in [40], [41] cannot be used as a detector for isomers. Additionally, in multiple access, user fairness is always one of the key issues to be addressed. In multiple access systems, using different types of molecules with non-differential diffusion coefficients to distinguish users imposes the challenge to coordinate the performance between strong and weak users. Against this background, therefore, in this paper, we propose a multi-user MC system based on MDMA, where multiple types of molecules with different diffusion coefficients are employed to serve users.

As in wireless communications, resource allocation among multiple nano-users for them to attain the best possible performance is an important optimization problem in MC systems. To address this issue, when given a limited energy budget, the authors of [42] proposed to maximize the channel capacity and data rate by adjusting the detection threshold and symbol duration. In [43], a game-theoretic framework was designed for distributed resource allocation in MC systems to achieve high system efficiency, while ensuring fairness among different nano-machines. To minimize the expected error probability of each hop, Arman *et al.* derived the optimal number of molecules released by the transmitter and the optimal detection threshold of the receiver in a multi-hop MC framework [44]. In a drug delivery system, to optimize the number of released molecules and symbol durations, the multi-objective optimizations were formulated in [30]. Moreover, constrained by the number of molecules available, which is caused by the finite availability of molecule synthesizing energy and limited storage capabilities of reservoir, the authors of [45] and [46] both optimized the molecular resource allocation among nano-users to improve the error performance for a cooperative MC system. Nevertheless, compared with the traditional multiple access in electromagnetic communication, the resource allocation issue in molecular multiple access networks has so far only received little research attention and in particular, for the multi-user networks with different diffusion coefficients, there are no published works found. Therefore, based on the proposed MDMA system, we study the optimization of molecular resource allocation, including the assignment of the types of molecules and the number of molecules of each of the types. The contributions of this paper are summarized as follows.

- We propose a novel MDMA system, where information molecules with different diffusion coefficients are employed to serve users. For signal detection, we derive a closed-form expression and find the approximately optimal detection threshold.
- We propose and investigate three different optimization criteria that lead to different problem formulations, including the min-max fairness for error probability, max-min fairness for achievable rate, and weighted sum rate maximization. Two assignment strategies for the types of molecules, i.e., best-to-best (BTB) and best-to-worst (BTW), are proposed. After the types of molecules are determined for all users, we optimize the number of molecules for each type of molecules, and correspondingly, provide the semi-closed solutions to the optimization problems.
- We perform Monte Carlo simulations to evaluate the effectiveness of the proposed resource allocation methods with different optimization objectives. Simulation results show that the combination of BTW and the optimal allocation of the number of molecules can exhibit better performance than other schemes.

The remainder of the paper is organized as follows. In Section II, we describe the proposed multi-user MC system and introduce various resource optimization problems. Section III details the joint resource allocation for all considered optimizat ion objectives. The performance of the proposed assignment strategies is evaluated in Section IV, and finally, the conclusion is drawn in Section V.

II. Problem Statement

A. System Model

Based on the MDMA technology, in this section, we consider a multi-user downlink diffusion MC system, which consists of a point transmitter and K spherical passive receivers/users, as illustrated in Fig. 1. For implementation of the considered scenario, we assume that a transmitter can store (or generate) K types of information molecules for communicating with the K users, and the k-th spherical passive receiver or user u_k is capable of recognizing and distinguishing a specific

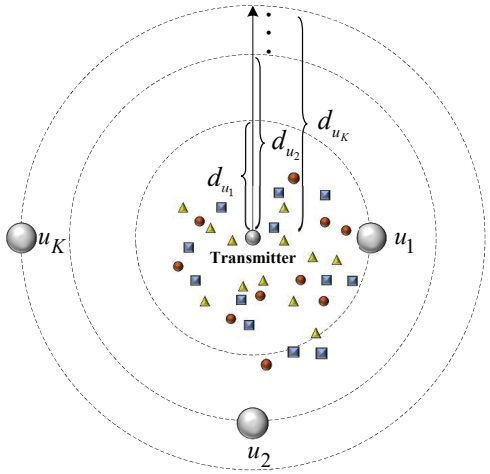

Fig. 1. The schematic diagram for multi-user downlink transmission scenario.

type of molecules via, such as the sensors attached with the receiver, where $k = 1, 2, \cdots, K$. Different from the conventional multi-user or multiple-molecules MC systems [33–39], in this paper, we relax the assumption that all molecules have a common diffusion coefficient, even though this is reasonable for isomers. Instead, we assume that different types of molecules may have different diffusion coefficients. Therefore, in the considered system, we employ K types of molecules $\{M_1, M_2, \cdots, M_K\}$ with the diffusion coefficients $\{D_1, D_2, \cdots, D_K\}$ to serve users $\{u_1, u_2, \cdots, u_K\}$. Without loss of generality, we assume that $D_1 \leq D_2 \leq \cdots \leq D_K$ and $d_{u_1} \leq d_{u_2} \leq \cdots \leq d_{u_K}$, where d_{u_k} represents the transmission distance from the transmitter to the center of the k-th user for $k = 1, 2, \cdots, K$. Moreover, it is also assumed that the receiving capability of all users is the same, i.e, $V_{u_1} = V_{u_2} = \cdots = V_{u_K}$ or $r_{u_1} = r_{u_2} = \cdots = r_{u_K}$, where V_{u_k} and r_{u_k} denote the volume and radius of the k-th user, respectively. According to the fact described in [47] that the concentration of molecules inside the passive receiver can be well approximated as uniform distribution when the radius of the receiver is no more than 15% of the distance from the center of the receiver to the transmitter, we can define the probability of observing a given M_{u_k} molecule, emitted from the transmitter at $t = 0$, inside V_{u_k} at time t as

$$p_{u_k}(t)=\begin{cases} \frac{V_{u_k}}{\left(4\pi D_{u_k} t\right)^{3/2}} e^{\left(-\frac{d_{u_k}^2}{4D_{u_k}t}\right)}, & \text{if } \frac{r_{u_k}}{d_{u_k}} \leq 0.15 \\ \frac{1}{2}\left(\operatorname{erf}\left(\tau_1\right)+\operatorname{erf}\left(\tau_2\right)\right) & \\ +\frac{\sqrt{D_{u_k}t}}{d_{u_k}\sqrt{\pi}}\left(e^{-\tau_1^2}-e^{-\tau_2^2}\right), & \text{if } \frac{r_{u_k}}{d_{u_k}} > 0.15 \end{cases}. \quad (1)$$

Here, $\tau_1 = \frac{r_{u_k}+d_{u_k}}{2\sqrt{D_{u_k}t}}$, $\tau_2 = \frac{r_{u_k}-d_{u_k}}{2\sqrt{D_{u_k}t}}$, and D_{u_k} is the diffusion coefficient of type M_{u_k} molecules, where $M_{u_k} \in \{M_1, M_2, \cdots, M_K\}$ denotes the type of molecules assigned to u_k for $k \in \{1, 2, \cdots, K\}$.

During the diffusion phase in an unbounded 3-dimensional (3-D) environment, it is assumed that the transmitter can emit K types of molecules simultaneously and all information molecules do not react with each other. For simplicity, in this work, we consider that the ON/OFF keying (OOK) modulation is used to map the user information, which can be represented by a binary information sequence, i.e.,

$$\boldsymbol{x}_{u_k} = \left\{x_{u_k}^{(1)}, x_{u_k}^{(2)}, \cdots, x_{u_k}^{(l)}, \cdots\right\}, \quad (2)$$

where $x_{u_k}^{(l)} \in \{0, 1\}$ is the l-th symbol of user u_k conveyed by the transmitter. Per the rules of OOK, the transmitter releases Q_{u_k} molecules of type M_{u_k} to convey information symbol "1" for user u_k, and releases no molecules of type M_{u_k} to convey information symbol "0". Then, when $lT_s < t < (l+1)T_s$, where T_s is the symbol duration, the number of type M_{u_k} molecules measured by user u_k can be expressed as

$$y_{u_k}^{(l)}(t) = \sum_{j=1}^{l} Q_{u_k}\left[p_{u_k}(t - jT_s) + n_{u_k}^{(j)}(t)\right] x_{u_k}(j), \quad (3)$$

where $n_{u_k}^{(j)}(t)$ is the counting noise due to the transmission of a molecule for the j-th symbol, which takes into account of the distortion unpredictable by the Fick's law of diffusion. Additionally, as seen in (3), the terms corresponding to $j = 1, \cdots, l-1$ generate ISI on the transmission of the l-th symbol.

As shown in [48], when an impulse of molecules is emitted at $t = 0$, the concentration reaches its peak at $t_{u_k} = d_{u_k}^2/6D_{u_k}$. In order to derive the expressions for detecting the l-th symbol, we assume that all users can be synchronized with the incoming signal[1], and are capable of sampling for the concentrations at $t = lT_s + \hat{t}_{u_k}$, where $\hat{t}_{u_k}$ is the estimate of t_{u_k}. Then, following [48, 53], it can be shown that the number of molecules observed within V_{u_k} at $t = lT_s + \hat{t}_{u_k}$ can be expressed as

$$\begin{aligned} y_{u_k}^{(l)} &= \sum_{j=1}^{l}\left[p_{u_k}([l-j]T_s + \hat{t}_{u_k}) + n_{u_k}^{(j)}(lT_s + \hat{t}_{u_k})\right] Q_{u_k} x_{u_k}^{(j)} \\ &= \sum_{j=1}^{l}\left[p_{u_k,l-j} + n_{u_k}^{(j)}(lT_s + \hat{t}_{u_k})\right] Q_{u_k} x_{u_k}^{(j)} \end{aligned} \quad (4)$$

where $p_{u_k,l-j} = p_{u_k}([l-j]T_s + \hat{t}_{u_k})$ for $l = 1, 2, \cdots$ and $k = 1, 2, \cdots, K$. When l is large, we should expect that the ISI imposed by the symbols sent well before the l-th symbol can be ignored. For this sake, let us assume that the maximum length of ISI is L symbols. Following [54], L can be determined by

$$L = \arg\max_i \left\{\frac{p_{u_k,i}}{p_{u_k,0}} \geq \xi\right\}, \quad (5)$$

where ξ is the percentage level that ISI can be ignored. By introducing the maximum length of ISI L, (4) can be expressed as

$$y_{u_k}^{(l)} = \sum_{j=\max\{1,l-L\}}^{l}\left[p_{u_k,l-j} + n_{u_k}^{(j)}(lT_s + \hat{t}_{u_k})\right] Q_{u_k} x_{u_k}^{(j)}. \quad (6)$$

[1]Several works aiming at the synchronization in MC have been proposed recently. As some examples, synchronization in MC can be achieved by means of external signals [49], [50], or a blind synchronization algorithm [51], [52].

Moreover, as discussed in [44, 55], in diffusive MC, $y_{u_k}^{(l)}$ can be well approximated by a Poisson random variable (R.V.), i.e.,

$$y_{u_k}^{(l)} \sim \mathcal{P}\left(\Lambda_{u_k}(l) = \sum_{j=\max\{1,l-L\}}^{l} \lambda_{u_k}(j) x_{u_k}^{(j)}\right), \quad (7)$$

where $\lambda_{u_k}(j) = Q_{u_k} p_{u_k,l-j}$. For simplicity, we define $\Lambda_{u_k,z}$ as the conditional mean when $x_{u_k}^{(l)} = z$, where $z \in \{0,1\}$.

According to [54], for OOK, the detection threshold relative to the peak $Q_{u_k} p_{u_k,0}$ can be written as

$$C_{T,u_k} = \alpha_{u_k} Q_{u_k} p_{u_k,0}, \quad (8)$$

where α_{u_k} can be referred to as the normalized threshold, and generally, $0 \le \alpha_{u_k} \le 1$. Furthermore, by comparing the corresponding observation with the threshold, the receiver can make the decision of a bit stream as

$$\hat{x}_{u_k}^{(l)} = \begin{cases} 1, & \text{when } y_{u_k}^{(l)} \ge C_{T,u_k} \\ 0, & \text{when } y_{u_k}^{(l)} < C_{T,u_k} \end{cases}, \quad (9)$$

where $k = 0, 1, \cdots, K$ and $l = 1, 2, \cdots$. Based on [56], assuming $l > L$, we can express the miss-probability P_{M,u_k} and the false-alarm probability P_{F,u_k} for user u_k as follows

$$\begin{aligned} P_{M,u_k} &= P\left(\hat{x}_{u_k}^{(l)} = 0 \mid x_{u_k}^{(l)} = 1\right) \\ &= \sum_{\boldsymbol{x}_{u_k}^L \in \beta^L} P\left(\boldsymbol{x}_{u_k}^L\right) P\left(y_{u_k}^{(l)} \le C_{T,u_k} \mid \boldsymbol{x}_{u_k}^L, x_{u_k}^{(l)} = 1\right), \quad (10) \\ P_{F,u_k} &= P\left(\hat{x}_{u_k}^{(l)} = 1 \mid x_{u_k}^{(l)} = 0\right) \\ &= \sum_{\boldsymbol{x}_{u_k}^L \in \beta^L} P\left(\boldsymbol{x}_{u_k}^L\right) P\left(y_{u_k}^{(l)} \ge C_{T,u_k} \mid \boldsymbol{x}_{u_k}^L, x_{u_k}^{(l)} = 0\right), \quad (11) \end{aligned}$$

where $\beta = \{0,1\}$, $\boldsymbol{x}_{u_k}^L = \left\{x_{u_k}^{(l-L)}, \ldots, x_{u_k}^{(l-1)}\right\}$ is the ISI sequence, and $P\left(\boldsymbol{x}_{u_k}^L\right)$ is the probability of the occurrence of a specific sequence of $\boldsymbol{x}_{u_k}^L$. When assuming that $P(0) = P(1) = 0.5$, we have $P\left(\boldsymbol{x}_{u_k}^L\right) = \frac{1}{2^L}$. Furthermore, we can use the probability mass function of $y_{u_k}^{(l)}$ with the Poisson distribution to obtain the closed-form expressions of P_{M,u_k} and P_{F,u_k}, i.e.,

$$P_{M,u_k} = \frac{1}{2^L} \sum_{\boldsymbol{x}_{u_k}^L \in \beta^L} \sum_{n=0}^{\lceil C_{T,u_k} \rceil} \frac{\Lambda_{u_k,1}^n e^{-\Lambda_{u_k,1}}}{n!}, \quad (12)$$

$$P_{F,u_k} = 1 - \frac{1}{2^L} \sum_{\boldsymbol{x}_{u_k}^L \in \beta^L} \sum_{n=0}^{\lceil C_{T,u_k} \rceil} \frac{\Lambda_{u_k,0}^n e^{-\Lambda_{u_k,0}}}{n!}. \quad (13)$$

The bit error rate (BER) of user u_k employing OOK modulation can be given by

$$\begin{aligned} P_{u_k} &= P\left(x_{u_k}^{(l)} = 1\right) P\left(\hat{x}_{u_k}^{(l)} = 0 \mid x_{u_k}^{(l)} = 1\right) \\ &\quad + P\left(x_{u_k}^{(l)} = 0\right) P\left(\hat{x}_{u_k}^{(l)} = 1 \mid x_{u_k}^{(l)} = 0\right) \\ &= \frac{1}{2}\left(P_{M,u_k} + P_{F,u_k}\right). \quad (14) \end{aligned}$$

Applying (12) and (13) into (14), the closed-form expression of BER for user u_k can be obtained. To the best of our knowledge, the values of thresholds in OOK impose a high impact on the BER performance. Therefore, it is necessary to derive the optimal C_{T,u_k} (or α_{u_k}). To find the optimal detection threshold, we take the discrete partial derivative of (14) with respect to C_{T,u_k}, which, in turn, requires the discrete partial derivative of (12) and (13) with respect to its first elementary variable, C_{T,u_k}. However, it is difficult to obtain the first discrete derivative of P_{M,u_k} and P_{F,u_k}, since they need to consider all possible $\boldsymbol{x}_{u_k}^L$ to obtain the corresponding $\Lambda_{u_k,1}$ and $\Lambda_{u_k,0}$. Given that ISI symbols are unknown for users, according to [57], we can approximate $\Lambda_{u_k,z}$ as $\bar{\Lambda}_{u_k,z}$, expressed as

$$\begin{aligned} \bar{\Lambda}_{u_k,z} &= E\left[\Lambda_{u_k,z}\right] \\ &= Q_{u_k}\left(\frac{1}{2} \sum_{j=\max\{1,l-L\}}^{l} p_{u_k,l-j} + z p_{u_k,0}\right), \quad (15) \end{aligned}$$

for $z \in \{0,1\}$. Furthermore, following [44], we can use the Stirling formula to approximate the factional term, i.e., $n! \simeq (2\pi n)^{1/2}(n/e)^n$. Moreover, based on the fact described on [44] that the discrete cumulative distribution function (CDF) of the Poisson R.V. can be approximated as a continuous CDF, P_{M,u_k} and P_{F,u_k} can be rewritten as

$$\begin{aligned} P_{M,u_k} &\simeq \int_0^{\lceil C_{T,u_k} \rceil} \frac{e^{\left(n-\bar{\Lambda}_{u_k,1}\right)}\left(\frac{\bar{\Lambda}_{u_k,1}}{n}\right)^{\left(n+\frac{1}{2}\right)}}{\sqrt{2\pi\bar{\Lambda}_{u_k,1}}} dn, \\ P_{F,u_k} &\simeq 1 - \int_0^{\lceil C_{T,u_k} \rceil} \frac{e^{\left(n-\bar{\Lambda}_{u_k,0}\right)}\left(\frac{\bar{\Lambda}_{u_k,0}}{n}\right)^{\left(n+\frac{1}{2}\right)}}{\sqrt{2\pi\bar{\Lambda}_{u_k,0}}} dn. \quad (16) \end{aligned}$$

Substituting the above equations into (14) can obtain its approximation, and the optimal C_{T,u_k} can be solved through taking the derivative of the approximate expression of (14) with respect to C_{T,u_k}, i.e.,

$$\lceil C_{T,u_k} \rceil = \frac{1}{\ln\left(\frac{\bar{\Lambda}_{u_k,1}}{\bar{\Lambda}_{u_k,0}}\right)}\left(\bar{\Lambda}_{u_k,1} - \bar{\Lambda}_{u_k,0}\right). \quad (17)$$

In other words, the optimal α_{u_k} can be defined as

$$\alpha_{u_k}^{opt} = \frac{1}{\ln\left(\frac{\bar{\Lambda}_{u_k,1}}{\bar{\Lambda}_{u_k,0}}\right)}. \quad (18)$$

To facilitate the analysis in the sequel, for large Q_{u_k}, we further approximate $y_{u_k}^{(l)}$ as a Gaussian R.V., expressed as

$$y_{u_k}^{(l)} \sim \mathcal{N}\left(\Lambda_{u_k}(l), \Lambda_{u_k}(l)\right). \quad (19)$$

By using the probability density function of $y_{u_k}^{(l)}$ with the Gaussian distribution, P_{M,u_k} and P_{F,u_k} can be expressed as

$$P_{M,u_k} = 1 - \frac{1}{2^L} \sum_{\boldsymbol{x}_{u_k}^L \in \beta^L} Q\left(\sqrt{Q_{u_k}}\eta_{u_k,1}\right), \quad (20)$$

$$P_{F,u_k} = \frac{1}{2^L} \sum_{\boldsymbol{x}_{u_k}^L \in \beta^L} Q\left(\sqrt{Q_{u_k}}\eta_{u_k,0}\right), \quad (21)$$

where

$$\eta_{u_k,0} = \frac{\left(\alpha_{u_k} p_{u_k,0} - p_{u_k,1} x_{u_k}^{(l-1)}\right)}{\sqrt{p_{u_k,1} x_{u_k}^{(l-1)}}}$$
$$\eta_{u_k,1} = \frac{\left(\left(\alpha_{u_k}-1\right) p_{u_k,0} - p_{u_k,1} x_{u_k}^{(l-1)}\right)}{\sqrt{\left(p_{u_k,0} + p_{u_k,1} x_{u_k}^{(l-1)}\right)}}, \quad (22)$$

and $Q(\cdot)$ denotes the Gaussian Q-function. Considering $0 \leq \alpha_{u_k} \leq 1$, we can find that $\eta_{u_k,1} \leq 0$ always holds; while for $\eta_{u_k,0}$, if

$$\alpha_{u_k} > \frac{p_{u_k,1}}{p_{u_k,0}} \quad (23)$$

is satisfied, $\eta_{u_k,0} > 0$. On one hand, according to (1), we can find $\frac{p_{u_k,1}}{p_{u_k,0}}$, the ratio of the ISI generated by previous symbols to the current symbol, is relatively small. Therefore, (23) can be easily satisfied, especially when the optimal α_{u_k} derived in (18) is employed. For clarity, in this paper, we assume $\eta_{u_k,1} \leq 0 < \eta_{u_k,0}$.

Applying (20) and (21) into (14), the closed-form expression of BER for user u_k can be updated

$$P_{u_k} = \frac{1}{2} + \frac{1}{2^{L+1}} \sum_{\boldsymbol{x}_{u_k}^L \in \beta^L} \left\{ Q\left(\sqrt{Q_{u_k}}\eta_{u_k,0}\right) - Q\left(\sqrt{Q_{u_k}}\eta_{u_k,1}\right)\right\}. \quad (24)$$

Afterwards, we can obtain the mutual information (rate) I_{u_k} for the k-th user as

$$I_{u_k} = \sum_{x_{u_k}^{(l)}, \hat{x}_{u_k}^{(l)} \in \beta} P\left(\hat{x}_{u_k}^{(l)} | x_{u_k}^{(l)}\right) P\left(x_{u_k}^{(l)}\right) \log_2 \frac{P\left(\hat{x}_{u_k}^{(l)} | x_{u_k}^{(l)}\right)}{P\left(\hat{x}_{u_k}^{(l)}\right)}. \quad (25)$$

Here, following the above derivation of the error probability, $P\left(\hat{x}_{u_k}^{(l)} | x_{u_k}^{(l)}\right)$ and $P\left(\hat{x}_{u_k}^{(l)}\right)$ involved in (25) can be acquired.

B. Problem Formulation

For a multi-user MC system with given environmental parameters, its performance relies on the molecular resource allocation, which includes the assignment for the types of molecules and the number of molecules for each of the types. In this paper, we investigate the optimization of molecular resource allocation for the proposed scheme in Section II-A. For this purpose, we consider the following optimization problems.

1) First, we impose the min-max fairness criterion to provide BER fairness for all users. The corresponding resource allocation problem is given by

$$\min_{Q_{u_1}, Q_{u_2}, \ldots, Q_{u_K}} \max\left\{P_{u_1}, P_{u_2} \cdots, P_{u_K}\right\}. \quad (26)$$

2) In addition to BER performance, user fairness can also be reflected by their achievable rates. Therefore, we can also use the max-min fairness criterion to achieve user fairness, which is mathematically expressed as

$$\max_{Q_{u_1}, Q_{u_2}, \ldots, Q_{u_K}} \min\left\{I_{u_1}, I_{u_2}, \cdots I_{u_K}\right\}. \quad (27)$$

3) Furthermore, in multi-user communication system, one of the well-known optimization objectives is to maximize the sum rate of all users. Additionally, to avoid that the resource is assigned to only a fraction of users, maximization of the weighted sum rates of all users can be considered [58]. Hence, in this paper, we consider the weighted sum rate maximization problem of

$$\max_{Q_{u_1}, Q_{u_2}, \cdots, Q_{u_K}} \sum_{k=1}^{K} \mu_{u_k} I_{u_k}$$
$$s.t. \;\; \mu_{u_k} > 0, \quad (28)$$

where μ_{u_k} is the weight for user u_k.

Additionally, achieving the above objectives should be under the constraint that the total number of molecules is a given number. However, within a symbol duration, the transmitted sequence $\left\{x_{u_1}^{(l)}, x_{u_2}^{(l)}, \cdots, x_{u_K}^{(l)}\right\}$ is unknown, indicating that the total number of molecules successfully emitted at the transmitter is not a constant. Therefore, we limit the average number of molecules released, i.e,

$$E\left[\sum_{k=1}^{K} Q_{u_k} x_{u_k}^{(l)}\right] \leq \bar{\mathcal{Q}}, Q_{u_k} > 0, \quad (29)$$

where $E[\cdot]$ is the expectation operation and $\bar{\mathcal{Q}}$ denotes the maximum average number of molecules released by the transmitter. Assuming $P\left(x_{u_k}^{(l)} = 0\right) = P\left(x_{u_k}^{(l)} = 1\right) = \frac{1}{2}$, (29) can be rewritten as

$$\sum_{k=1}^{K} Q_{u_k} \leq \mathcal{Q}, Q_{u_k} > 0, \quad (30)$$

where $\mathcal{Q} = 2\bar{\mathcal{Q}}$ is the total number of molecules released per transmission.

III. Optimization Analysis

Note that in the proposed system, the optimization for the allocation of types of molecules and the associated number of associated molecules is, unfortunately, a mixed problem, which is not convex. Finding the jointly optimal solution requires an exhaustive search, which results in prohibitive computational complexity. Therefore, in practice, we tend to first fix the assignment for the types of molecules and then optimize the number of molecules assigned to different types. Moreover, per the corresponding optimization criterion, we can obtain the optimal solutions from all possible combinational allocation strategies, which can also be referred to as the jointly suboptimal allocation strategy. Hence, to reduce the complexity, in this section, we only consider the received signal composing of the current and previously transmitted symbol, yielding $\Lambda_{u_k}(l) = \lambda_{u_k}(l) x_{u_k}^{(l)} + \lambda_{u_k}(l-1) x_{u_k}^{(l-1)}$. Furthermore, for simplicity, we take $K = 2$ as an example to illustrate the principles of molecular resource allocation, while the general optimization analysis for the multi-user scenario will be detailed in *Remark*.

A. Optimization for Min-Max Fairness

In this subsection, we consider the molecular resource allocation to achieve the BER fairness in the proposed scheme. First, when information molecules are fixed for all users, we can list all the possible allocation strategies, i.e., BTW and BTB. With the BTW, the best type of molecules with the largest diffusion coefficient is assigned to the worst user with the maximum transmission distance, the second best type to second worst user, and so on. By contrast, when BTB is employed, the allocation of types of molecules to users is opposite to BTW, i.e., best type to best user and worst type to worst user.[2] After allocation of the types of molecules to users, then, we can derive the optimal allocation results for the number of molecules to different users. Moreover, by comparing the performance of the BTB and BTW associated with the allocation of the number of molecules, the jointly suboptimal allocation strategy can be determined.

1) Best-To-Worst (BTW): Assuming that the BTW scheme is employed in the proposed system, we have $D_{u_k} = D_k$ for $k = 1, 2, \ldots, K$. According to the aforementioned, we can rewrite (26) for $K = 2$ as

$$\begin{aligned} &\min_{\rho} \max \left\{P_{u_1}, P_{u_2}\right\} \\ &s.t. \quad Q_{u_1} + Q_{u_2} \leq \rho\mathcal{Q} + (1-\rho)\,\mathcal{Q} = \mathcal{Q}, \\ &\qquad 0 < \rho < 1, \end{aligned} \tag{31}$$

where $\rho\mathcal{Q}$ and $(1-\rho)\mathcal{Q}$ are the number of molecules allocated to users u_1 and u_2, respectively, and ρ is the allocation coefficient.

Proposition 1: Suppose that type $M_1(M_2)$ molecules serves user $u_1(u_2)$. Then, the optimal solution to (31) is given by $\rho = \rho_{opt}$, where ρ_{opt} can be obtained through solving the following equation

$$\sum_{k\in\{1,2\}} (-1)^{k+1} \left\{P_{M,u_k} + P_{F,u_k}\right\} = 0. \tag{32}$$

Considering it is mathematically intractable to derive a closed-form expression for ρ_{opt} from (32), we resort to the bisection method or Newton iterative methods to solve (32) and obtain ρ_{opt}. Note that this operation is still applicable to (34) and (37) to solve ρ_{opt}.

Proof: See Appendix A. ∎

2) Best-To-Best (BTB): In the context of BTB scheme, we have the k-th user served by type M_{K-k+1} molecules for $k = 1, 2, \cdots, K$. Following the derivation of the BTW scheme, the optimal allocation coefficient $\rho = \rho_{opt}$ can be obtained by solving (32) with setting $D_{u_k} = D_{K-k+1}$.

Finally, we determine the jointly suboptimal allocation strategy by first applying all the optimal ρ to $\max\left\{P_{u_1}, P_{u_2}\right\}$, and then comparing the values among all $\max\left\{P_{u_1}, P_{u_2}\right\}$. The allocation strategy attaining the smallest $\max\left\{P_{u_1}, P_{u_2}\right\}$ represents a better allocation.

[2]If some users have the same transmission distance or some types of molecules have the same diffusion coefficients in the proposed scheme, random ordering for these users or these types of molecules will be performed.

B. Optimization for Max-Min Fairness

Similar to the optimization for min-max fairness, we first employ the BTW scheme to assign the information molecules, yielding $D_{u_k} = D_k$ for $k = 1, 2, \cdots, K$. For $K = 2$, (27) can be re-written as

$$\begin{aligned} &\max_{\rho} \min\left\{I_{u_1}, I_{u_2}\right\} \\ &s.t. \quad Q_{u_1} + Q_{u_2} \leq \rho\mathcal{Q} + (1-\rho)\,\mathcal{Q} = \mathcal{Q}, \\ &\qquad 0 < \rho < 1. \end{aligned} \tag{33}$$

Proposition 2: Suppose that type $M_1(M_2)$ molecules serves user $u_1(u_2)$. Then, the optimal solution to (33) is given by $\rho = \rho_{opt}$, where ρ_{opt} yields

$$\begin{aligned} \sum_{k\in\{1,2\}} (-1)^{k+1} \{&P_{M,u_k} \log_2 \mathcal{M}_k \\ &+ P_{F,u_k} \log_2 \mathcal{F}_k + \log_2 \mathcal{T}_k\} = 0, \end{aligned} \tag{34}$$

where

$$\begin{aligned} \mathcal{M}_k &= \frac{P_{M,u_k}\left(1 - P_{M,u_k} + P_{F,u_k}\right)}{\left(1 - P_{F,u_k} + P_{M,u_k}\right)\left(1 - P_{M,u_k}\right)}, \\ \mathcal{F}_k &= \frac{P_{F,u_k}\left(1 - P_{F,u_k} + P_{M,u_k}\right)}{\left(1 - P_{M,u_k} + P_{F,u_k}\right)\left(1 - P_{F,u_k}\right)}, \\ \mathcal{T}_k &= \frac{4\left(1 - P_{F,u_k}\right)\left(1 - P_{M,u_k}\right)}{\left(1 - P_{F,u_k} + P_{M,u_k}\right)\left(1 - P_{M,u_k} + P_{F,u_k}\right)}. \end{aligned} \tag{35}$$

Proof: See Appendix B. ∎

Following the above procedure, the optimal ρ in case of BTB can also be obtained. Finally, the jointly suboptimal allocation strategy can be obtained by comparing the values of I_{u_1} (or I_{u_2}) when BTB and BTW are respectively employed. In other words, the jointly suboptimal allocation strategy is given by the combination of the assignment method for the types of molecules that yields the largest I_{u_1} and the associated ρ_{opt} for allocation of the number of molecules to each of the two types.

C. Optimization for Sum Rate Maximization

According to (28), when given the assignment for the types of molecules to $K = 2$ users under the BTW scheme, the problem of maximizing the weighted sum rate can be described as

$$\begin{aligned} &\max_{\rho} \mu_{u_1} I_{u_1} + \mu_{u_2} I_{u_2} \\ &s.t. \quad Q_{u_1} + Q_{u_2} \leq \rho\mathcal{Q} + (1-\rho)\,\mathcal{Q} = \mathcal{Q}, \\ &\qquad \left\{\mu_{u_1}, \mu_{u_2}\right\} > 0,\ 0 < \rho < 1. \end{aligned} \tag{36}$$

Proposition 3: Assume that type $M_1(M_2)$ molecules serves user $u_1(u_2)$. Then, the optimal solution to (36) is given by $\rho = \rho_{opt}$ with ρ_{opt} satisfying

$$\sum_{k\in\{1,2\}} \left\{\frac{P'_{M,u_k}}{2} \log_2 \mathcal{M}_k + \frac{P'_{F,u_k}}{2} \log_2 \mathcal{F}_k\right\} = 0. \tag{37}$$

Proof: See Appendix C. ∎

Similarly, we can also derive the optimal ρ when the BTB scheme is employed to assign the two types of molecules to the two users. Moreover, by comparing the results obtained by the

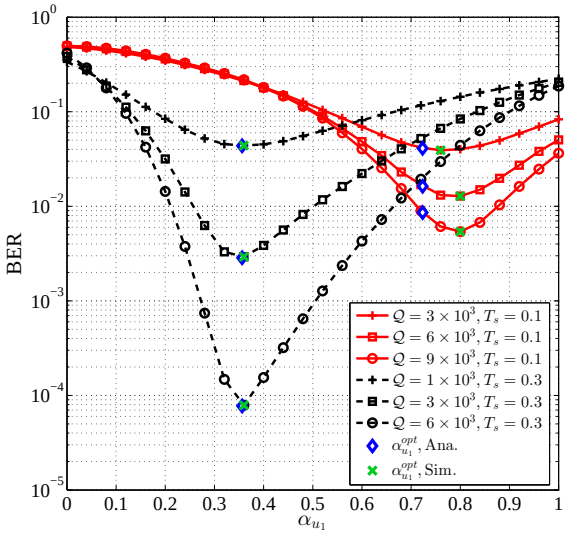

Fig. 2. BER performance of user u_1 as a function of the normalized detection threshold α_{u_1}, where $D_{u_1} = 3 \times 10^{-9} m^2/s$.

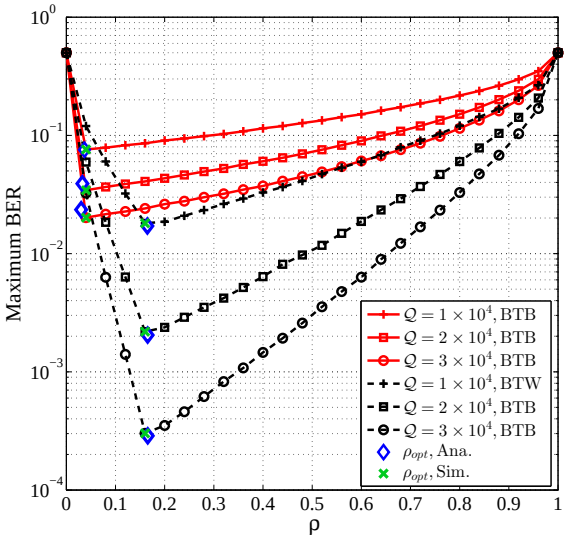

Fig. 3. Maximum BER performance of a two-user system as a function of the allocation coefficient ρ.

TABLE I
SYSTEM PARAMETERS

Parameter	Value
Symbol duration (T_s)	0.3s
Radius of receiver (r_{u_k})	$5\mu m$
Weight of user u_k (μ_k)	1
The percentage level ISI ignored (ξ)	0.01
Distance between transmitter and user u_1 (d_{u_1})	$20\mu m$
Distance between transmitter and user u_2 (d_{u_2})	$35\mu m$
Distance between transmitter and user u_3 (d_{u_3})	$45\mu m$
Diffusion coefficient of molecule M_1 (D_1)	$3 \times 10^{-9} m^2/s$
Diffusion coefficient of molecule M_2 (D_2)	$10 \times 10^{-9} m^2/s$
Diffusion coefficient of molecule M_3 (D_3)	$15 \times 10^{-9} m^2/s$

BTB and BTW schemes with the associated optimal values of ρ, we can find the jointly suboptimal allocation strategy under the considered situations.

Remark: When $K > 2$, it is clear that we are unable to obtain a closed-form expression for the optimal ρ in the above optimization problems. In the general case of K users, there are $K!$ possible assignment ways for types of molecules. The jointly optimal or suboptimal allocation strategy can only be obtained via exhaustive search, whose computational complexity is extreme, if the value of K is relatively large. In Section V, we will take $K = 3$ as an example to perform the optimization analysis through the numerical results and prove that the BTB and BTW schemes are capable of providing the lower and upper performance bounds on the systems with different optimization objectives, when the optimal allocation for $\mathcal{Q}$ is employed for all assignment strategies about types of molecules.

IV. NUMERICAL RESULTS

In this section, performance results are obtained with the aid of Monte Carlo simulations to verify the feasibility of the proposed resource optimization method. In our simulations, we consider both the two-user and three-user scenarios to perform the optimization analysis, in which the detailed system parameters are listed in Table I. For comparison, in the following, we also consider the equal allocation of the number of information molecules, i.e., $\rho_k = \frac{1}{K}$, as the baseline cases, noted as "Equal BTB/BTW" in the figures. Correspondingly, the optimal allocation of the number of information molecules is noted as "Optimal BTB/BTW". Note that for all simulation results or predefined detection thresholds, we use (5) to determine the maximum ISI length L; while for the optimization analysis in Section III, we set $L = 1$.

A. Validation of Optimal Detection Threshold

In this subsection, we take user u_1 as an example to assess the accuracy of the optimal normalized detection threshold $\alpha_{u_1}^{opt}$ derived from (18). First, Fig. 2 shows that both the theoretical and simulated $\alpha_{u_1}^{opt}$ are almost independent of the total number of transmitted molecules $\mathcal{Q}$, but inversely proportional to the symbol duration T_s, corroborating the conclusion in [54]. Moreover, we can observe that when $T_s = 0.1s$, the theoretical $\alpha_{u_1}^{opt}$ is not consistent with the simulated counterpart, with an error of about 9%. As T_s goes large to 0.3, we can see that the analytical $\alpha_{u_1}^{opt}$ perfectly matches to the simulated value due to the reduced effect of ISI. Therefore, for accuracy, we set $T_s = 0.3s$ in the sequel. Alternatively, the theoretically optimal α_{u_k} is employed in all simulations.

B. Two-User Optimization

In this subsection, we perform the optimization analysis for a two-user scenario, when assuming that type M_1 molecules and type M_2 molecules are deployed. Specifically, for BTB, we have $D_{u_1} = D_2$ and $D_{u_2} = D_1$; for BTW, let $D_{u_1} = D_1$ and $D_{u_2} = D_2$. Moreover, for clarity, we use the bisection

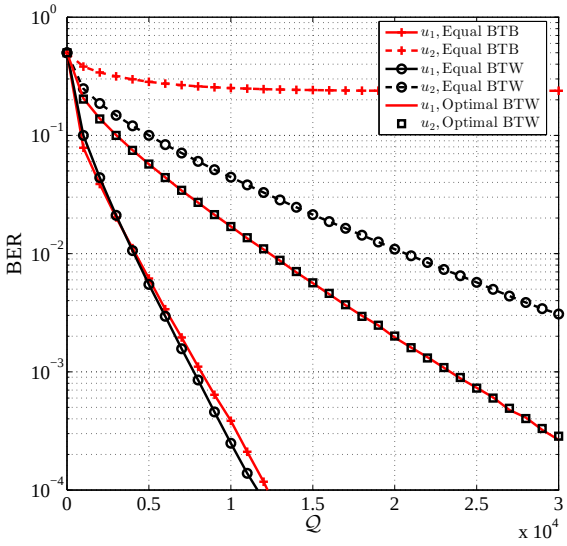

Fig. 4. BER performance comparison of "Equal BTB/BTW" and "Optimal BTB/BTW" with the total number of transmitted molecules $\mathcal{Q}$.

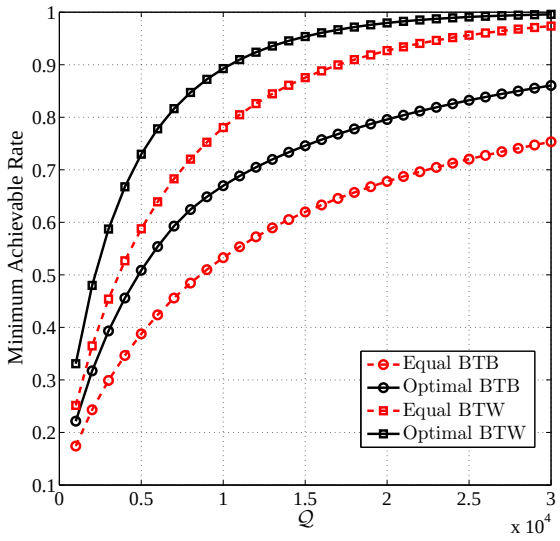

Fig. 5. Comparison of minimum achievable rate of "Equal BTB/BTW" and "Optimal BTB/BTW".

method to obtain the optimal allocation coefficients ρ_{opt} for all optimization objectives.

In Figs. 3 and 4, we demonstrate the optimization for min-max fairness on BER. Specifically, Fig. 3 shows the maximum BER performance of a two-user system as a function of the allocation coefficient ρ. From Fig. 3, we can find that similar to $\alpha_{u_1}^{opt}$, the optimal allocation coefficient is nearly the same for different $\mathcal{Q}$ values, explaining that the optimal allocation coefficients is robust to the number of emitted molecules per symbol. Moreover, it is clear that the analytical ρ_{opt} agrees well with the simulation counterparts for both BTB and BTW, validating the effectiveness of (32). However, we should note that the accuracy of ρ_{opt} is inversely proportional to the ISI length L. Furthermore, Fig. 3 depicts that BTW with the optimal allocation coefficient performs better than BTB also with optimal allocation coefficient. This can be understood by the fact that the maximum BER performance for a two-user system is always dominated by the worse user. In this subsection, we can regard user u_2 with the longer transmission distance as the worse user. With BTW, we assign the types of molecules with the larger diffusion coefficient (i.e., type M_2) to user u_2, which mitigates the BER performance degradation caused by the longer communication distance. By contrast, in BTB, the performance of user u_2 deteriorates rapidly, and may become unable to guarantee the normal communication. This is because the longer transmission distance and a smaller diffusion coefficient (D_1) make it very difficult for the number of molecules to reach the detection threshold within a symbol duration.

To further investigate the performance of the optimal BTW, in Fig. 4, we compare the optimal BTW and "Equal BTW/BTW", where $\rho_{opt} = 0.16$. As can be seen from Fig. 4, when the optimal BTW strategy is employed, the BER curve of user u_1 perfectly matches with that of user u_2, corroborating the proof of ***Proposition 1*** and achieving the ideal user fairness in terms of BER. As for the benchmarks, we can find that the gap between the two users' performance is large. Specifically, at BER $= 10^{-2}$, the performance gap is about 1.5×10^4 molecules for the equal BTW. Furthermore, for the equal BTB, error floor occurs for user u_2 at BER ≈ 0.5. We thereby conclude that for the optimization of min-max fairness, the best allocation strategy is the BTW with the optimal allocation for $\mathcal{Q}$.

Figure 5 depicts the minimum achievable rate of a two-user system using the optimal/euqal BTB/BTW, where the optimal allocation coefficients $\rho_{opt(s)}$ calculated by (34) are 0.04 and 0.16, respectively, for BTB and BTW. Similarly, ρ_{opt} under the max-min fairness criterion is independent of $\mathcal{Q}$. As expected, all BTW schemes outperform the corresponding BTB, which is also because user u_2 in BTW can obtain a relatively large diffusion coefficient to compensate for the defect of long transmission distance, when compared with user u_2 in BTB. Moreover, it is clearly seen that due to the use of optimal allocation for $\mathcal{Q}$, the optimal BTB/BTW is better than the equal allocation counterparts. We also note that the performance gap between the optimal and equal BTW is tailing off gradually as $\mathcal{Q}$ increases. In summary, the optimal BTW is capable of realizing a better performance under the max-min fairness rule.

In Fig. 6, we plot the sum rate of a two-user system using BTB/BTW versus the allocation coefficient ρ for different values of $\mathcal{Q}$. Unlike ρ_{opt} for the pervious optimization objectives, ρ_{opt} decreases with the increase of $\mathcal{Q}$ when maximizing the sum rate is considered. This can be understood by the following facts: 1) as $\mathcal{Q}$ goes larger, user u_1 can reach the limit of mutual information with a smaller allocation coefficient ρ; 2) to maximize the sum rate, user u_2 will be assigned a larger number of molecules to improve its data rate, i.e., increasing $1 - \rho_{opt}$. For the same reason clarified earlier, the obtained results show that BTW attains better sum rate performance

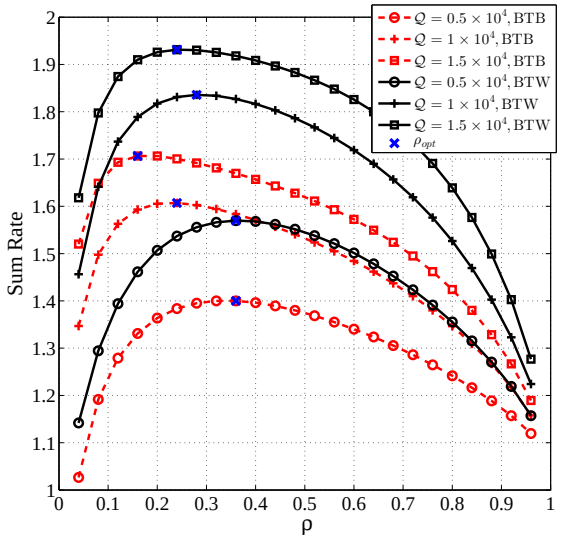

Fig. 6. Sum rate of the two-user system as a function of the allocation coefficient ρ.

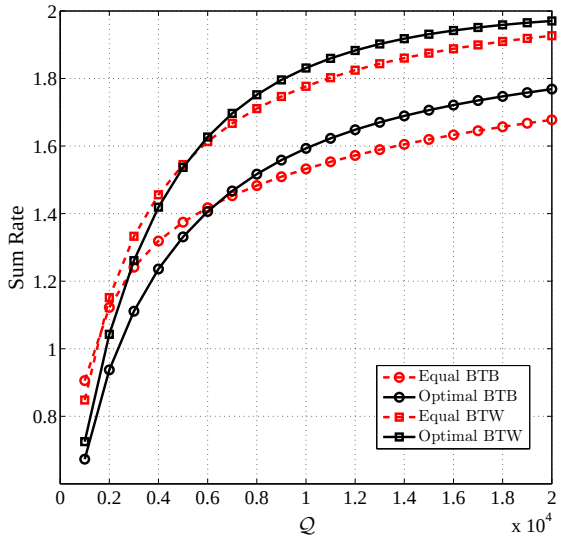

Fig. 7. Sum rate comparison of "Equal BTB/BTW" and "Optimal BTB/BTW".

than BTB for all considered $\mathcal{Q}$. Meantime, Fig. 6 reveals that the sum rate function is concave with respect to the allocation coefficient ρ both for BTB and BTW.

To illustrate the performance characteristics of BTB/BTW, in Fig. 7, we further compare the sum rate achieved by the optimal BTB/BTW and that achieved by the equal BTB/BTW schemes. One can observe that the optimal BTW exhibits the maximum sum rate, while the equal BTB performs worse, when $\mathcal{Q} \geq 0.7\times10^4$. Compared with the equal BTB/BTW, the reason for the performance loss of the optimal counterparts is that considering ρ_{opt} is a variable with respect to $\mathcal{Q}$, we select ρ_{opt} when $\mathcal{Q} = 1.5 \times 10^4$ as a globally optimal allocation coefficient for all $\mathcal{Q}$. Specifically, ρ_{opt} is set to 0.16 and 0.24, respectively, for BTB and BTW.

In summary, numerical results in Figs. 3-7 show that the best resource allocation among the considered schemes is the BTW with the optimal allocation for $\mathcal{Q}$. With the aid of the ρ_{opt} provided in ***Propositions 1-3***, the jointly suboptimal resource allocation strategy for a two-user system can be predesigned to enhance system's performance, either user fairness or sum rate.

C. Multi-User Optimization

In this subsection, we focus on a three-user network (i.e. users u_1, u_2, and u_3) to perform the optimization analysis. Note agian that the basic simulation parameters are listed in Table I. Moreover, ρ_1 and ρ_2 denote the allocation coefficients of the numbers of released molecules for users u_1 and u_2, respectively, and we also have $0 \leq \rho_1 + \rho_2 \leq 1$. Hence, the allocation coefficient of user u_3 is $1-(\rho_1+\rho_2)$.

Figure 8 depicts the maximum BER of the three-user network with all possible assignment strategies for the types of molecules, where the detailed strategies are given in Table II. From Fig. 8, we can find the minimum value of the maximum BER, and thus obtain the optimal allocation about $\mathcal{Q}$ for all

TABLE II
ALL POSSIBLE ASSIGNMENT RULES FOR TYPES OF MOLECULES

Assignment strategy	Molecular type for users		
	User u_1	User u_2	User u_3
BTW	M_1	M_2	M_3
Matching 1	M_1	M_3	M_2
Matching 2	M_2	M_1	M_3
Matching 3	M_2	M_3	M_1
Matching 4	M_3	M_1	M_2
BTB	M_3	M_2	M_1

users. For clarity, in Fig. 9, we further employ the optimal allocation coefficients ρ_1 and ρ_2 obtained from Fig. 8 to investigate the performance of all assignment strategies. As anticipated, the BTB and BTW schemes provide the lower and upper bounds on the performance for the considered system, when the optimal allocation for $\mathcal{Q}$ is employed for all assignment strategies about types of molecules. However, different from the two-user network, the optimal allocation for $\mathcal{Q}$ cannot be pre-designed via a detailed expression in a multi-user system. To effectively obtain the optimal ρ_1 and ρ_2 in BTB/BTW, it is necessary to introduce some initialization procedures. Moreover, for the remaining two optimization objectives, we can also acquire a similar conclusion as described in Fig. 9, i.e., the performances of the BTW and BTB schemes with the optimal allocation for $\mathcal{Q}$ are the upper and lower bounds of the system performance. This is accounted for the fact that for the optimization objectives considered in our work, the system performance is mainly determined by worse users, and thereby how to improve the performance of these users is the focus of our optimization. The BTB and BTW denote two extreme matching strategies for worse users, i.e., the worst and best matching. Specifically, the BTW can mitigate the performance loss of worse users by employing the types of molecules with larger diffusion coefficients, while the BTB further lowers the performance of these users.

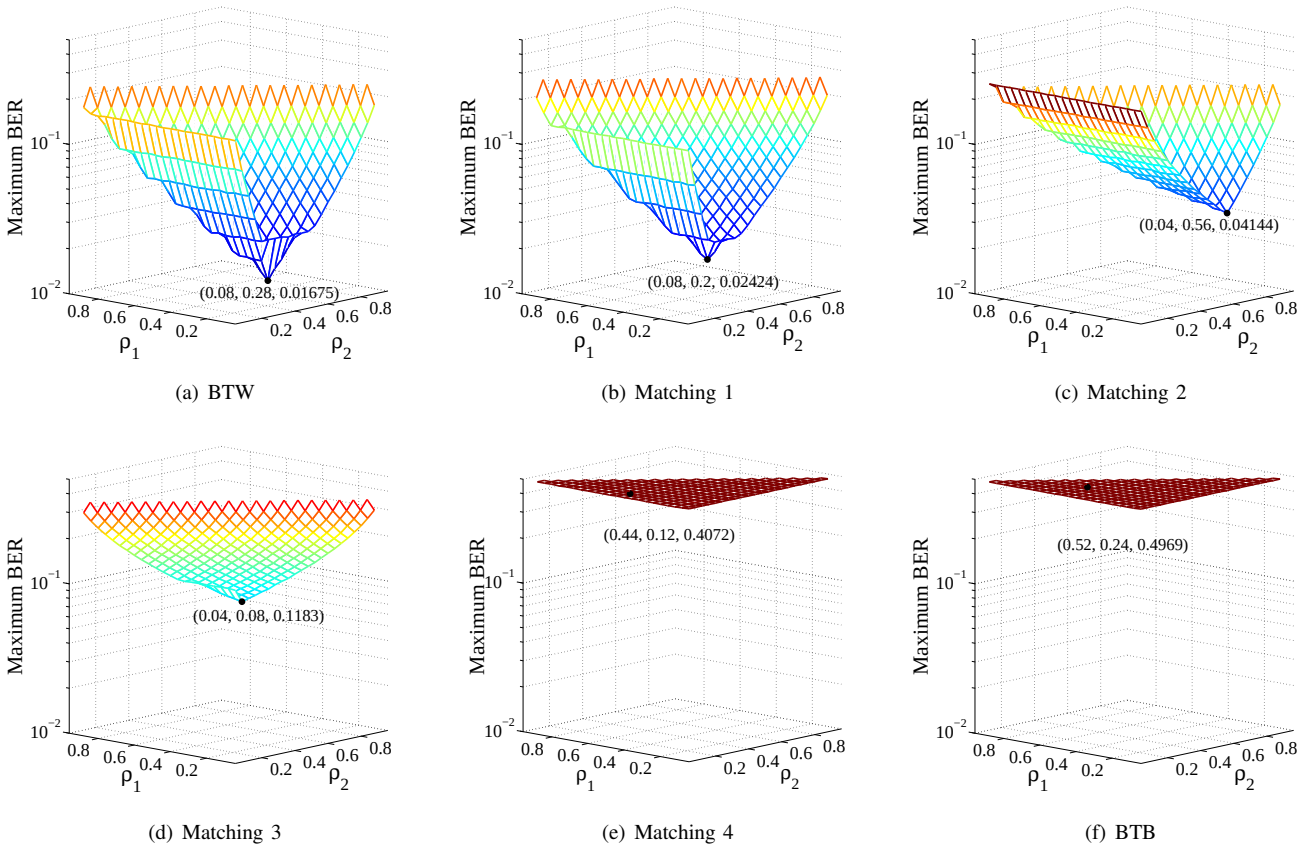

(a) BTW (b) Matching 1 (c) Matching 2

(d) Matching 3 (e) Matching 4 (f) BTB

Fig. 8. Maximum BER performance of a three-user system versus the allocation coefficients ρ_1 and ρ_2, where all possible molecule assignment strategies are considered and $\mathcal{Q} = 3 \times 10^4$.

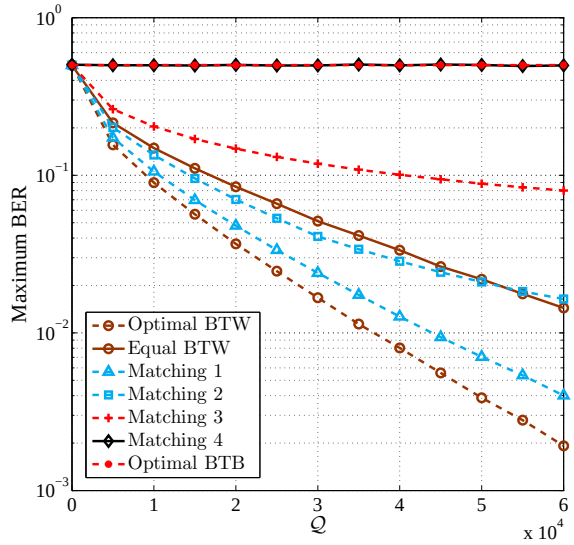

Fig. 9. Maximum BER of a three-user network as a function of the total number of released information molecules $\mathcal{Q}$.

V. Conclusion

In this paper, we investigated the molecular resource allocation for the MDMA-based MC systems, in which the information molecules with different diffusion coefficients are considered. For the proposed system, we considered three kinds of performance measures to obtain the jointly suboptimal allocation for the types of molecules and the associated number of molecules per type. Specifically, two assignment strategies, namely BTB and BTW, for the types of molecules were considered. Furthermore, for a two-user scenario, we provided the semi-closed form solutions to the optimal allocation of numbers of molecules for different optimization objectives with BTW/BTB. By contrast, in the three-user cases, we verified that the BTB and BTW with the optimal allocation of numbers of molecules are capable of providing the lower and upper bounds on the system's performance. Finally, numerical results illustrated that the jointly suboptimal allocation method among those considered is the BTW scheme associated with the optimal allocation of the number of emitted molecules.

Appendix A

From the principles of min-max (or max-min) based allocation [58–60], we can know that the allocation coefficient ρ satisfying $P_{u_1} = P_{u_2}$ is optimal, i.e., $\rho = \rho_{opt}$ when $P_{u_1} = P_{u_2}$, where P_{u_1} and P_{u_2} are given in (24). Therefore, the only thing we need to do is to verify the presence of ρ_{opt}.

The first step is to investigate the monotonicity of P_{u_1} and P_{u_2} with respect to the allocation coefficient ρ, which can be determined by checking whether its first derivative with

respect to its variable (i.e., ρ) is positive or not. Taking the first derivative of P_{u_1} with respect to ρ, we can obtain the following equation

$$\frac{dP_{u_1}}{d\rho} = \frac{1}{4}\sum_{x_{u_1}^{(l-1)}\in\beta}\sqrt{\frac{\mathcal{Q}}{8\rho\pi}}\Big(\eta_{u_1,1}e^{-\frac{1}{2}\rho\mathcal{Q}\eta_{u_1,1}^2} - \eta_{u_1,0}e^{-\frac{1}{2}\rho\mathcal{Q}\eta_{u_1,0}^2}\Big). \quad (38)$$

Considering $\eta_{u_1,1} \le 0 < \eta_{u_1,0}$, we thereby obtain

$$\eta_{u_1,0}e^{-\frac{1}{2}\rho\mathcal{Q}\eta_{u_1,0}^1} > \eta_{u_1,1}e^{-\frac{1}{2}\rho\mathcal{Q}\eta_{u_1,1}^2},\ \forall x_{u_1}^{(l-1)} \in \beta. \quad (39)$$

Applying the above equation to (38), we can obtain $\frac{dP_{u_1}}{d\rho} < 0$, indicating that P_{u_1} is degraded with the growth of ρ.

For P_{u_2}, we can use a similar method to analyze its monotonicity. First, the first derivative of P_{u_2} with respect to ρ is given by

$$\frac{dP_{u_2}}{d\rho}=\frac{1}{4}\sum_{x_{u_2}^{(l-1)}\in\beta}\frac{\sqrt{\mathcal{Q}}}{\sqrt{8\pi\left(1-\rho\right)}}\Big(\eta_{u_2,0}e^{-\frac{1}{2}(1-\rho)\mathcal{Q}\eta_{u_2,0}^2} - \eta_{u_2,1}e^{-\frac{1}{2}(1-\rho)\mathcal{Q}\eta_{u_2,1}^2}\Big). \quad (40)$$

For $\eta_{u_2,1} \le 0 < \eta_{u_2,0}$, we also obtain

$$\eta_{u_2,0}e^{-\frac{1}{2}\rho\mathcal{Q}\eta_{u_2,0}^2} > \eta_{u_2,1}e^{-\frac{1}{2}\rho\mathcal{Q}\eta_{u_2,1}^2},\ \forall x_{u_2}^{(l-1)} \in \beta, \quad (41)$$

and we thereby have $\frac{dP_{u_2}}{d\rho} > 0$. As a result, P_{u_2} is an increasing function of ρ.

Moreover, we need to find the values of P_{u_1} and P_{u_2}, respectively, when $\rho \to 0$ or $\rho \to 1$. Applying $\rho \to 0$ or $\rho \to 1$ into (24), we can easily obtain $\lim_{\rho\to 0} P_{u_1} = \lim_{\rho\to 1} P_{u_2} = \frac{1}{2}$. Meanwhile, since $Q\left(x\right)$ is a decreasing function, we have $Q\left(\sqrt{\rho\mathcal{Q}}\eta_{u_k,0}\right) - Q\left(\sqrt{\rho\mathcal{Q}}\eta_{u_k,1}\right) < 0$ for $\forall x_{u_k}^{(l-1)} \in \beta$ with $k = 1, 2$, and hence we can obtain $\lim_{\rho\to 1} P_{u_1} < \frac{1}{2}$ and $\lim_{\rho\to 0} P_{u_2} < \frac{1}{2}$.

Finally, considering that $\lim_{\rho\to 0} P_{u_1} > \lim_{\rho\to 0} P_{u_2}$, $\lim_{\rho\to 1} P_{u_1} < \lim_{\rho\to 1} P_{u_2}$, and the monotonicity of P_{u_1} and P_{u_2} about ρ, we can conclude that there is always $\rho = \rho_{opt}$ such that $P_{u_1} = P_{u_2}$.

Appendix B

First, we proof the monotonicity of I_{u_1} and I_{u_2} with respect to the variable ρ. Taking the first derivative of I_{u_k} with respect to ρ, we can obtain the following equation

$$\frac{dI_{u_k}}{d\rho} = \frac{P'_{M,u_k}}{2}\log_2\mathcal{M}_k + \frac{P'_{F,u_k}}{2}\log_2\mathcal{F}_k, \quad (42)$$

where for user u_1, we have

$$P'_{M,u_1} = \frac{1}{2}\sqrt{\frac{\mathcal{Q}}{8\pi}}\sum_{x_{u_1}^{(l-1)}\in\beta}\sqrt{\frac{1}{\rho}}\eta_{u_1,1}e^{-\frac{1}{2}\rho\mathcal{Q}\eta_{u_1,1}^2},$$
$$P'_{F,u_1} = -\frac{1}{2}\sqrt{\frac{\mathcal{Q}}{8\pi}}\sum_{x_{u_1}^{(l-1)}\in\beta}\sqrt{\frac{1}{\rho}}\eta_{u_1,0}e^{-\frac{1}{2}\rho\mathcal{Q}\eta_{u_1,0}^2}, \quad (43)$$

while for user u_2, we have

$$P'_{M,u_2} = -\frac{1}{2}\sqrt{\frac{\mathcal{Q}}{8\pi}}\sum_{x_{u_2}^{(l-1)}\in\beta}\sqrt{\frac{1}{1-\rho}}\eta_{u_2,1}e^{-\frac{1}{2}(1-\rho)\mathcal{Q}\eta_{u_2,1}^2}$$
$$P'_{F,u_2} = \frac{1}{2}\sqrt{\frac{\mathcal{Q}}{8\pi}}\sum_{x_{u_2}^{(l-1)}\in\beta}\sqrt{\frac{1}{1-\rho}}\eta_{u_2,0}e^{-\frac{1}{2}(1-\rho)\mathcal{Q}\eta_{u_2,0}^2}. \quad (44)$$

To proceed, we first investigate $\frac{dI_{u_1}}{d\rho}$. According to $\eta_{u_1,1} \le 0 < \eta_{u_1,0}$, we can obtain $P'_{M,u_1} < 0$ and $P'_{F,u_1} < 0$. Then, whether $\log_2\mathcal{M}_1$ and $\log_2\mathcal{F}_1$ are positive or negative, we can show that, if

$$P_{M,u_1} + P_{F,u_1} < 1, \quad (45)$$

both $\log_2\mathcal{M}_1$ and $\log_2\mathcal{F}_1$ are negative. This can be obtained by substituting (20) and (21) into (45) obtains

$$\sum_{x_{u_1}^{(l-1)}\in\beta} Q\left(\sqrt{Q_{u_1}}\eta_{u_1,0}\right) - Q\left(\sqrt{Q_{u_1}}\eta_{u_1,1}\right) < 0. \quad (46)$$

Since $\eta_{u_1,1} \le 0 < \eta_{u_1,0}$, (45) can be shown satisfied. As a result, we have $\frac{dI_{u_1}}{d\rho} > 0$, indicating that I_{u_1} is an increasing function with respect to ρ. Similarly, for the user u_2, we have $P'_{M,u_2} > 0$ and $P'_{F,u_1} > 0$ due to $\eta_{u_2,1} \le 0 < \eta_{u_2,0}$, and $\log_2\mathcal{M}_2$ and $\log_2\mathcal{F}_2$ can also be shown to be negative. Consequently, we can obtain that $\frac{dI_{u_2}}{d\rho} < 0$ and therefore I_{u_2} is degraded with the increase of ρ.

Moreover, we can prove that there is an intersection between I_{u_1} and I_{u_2}, i.e.,

$$\left(\lim_{\rho\to 0} I_{u_1}, \lim_{\rho\to 1} I_{u_1}\right) \cap \left(\lim_{\rho\to 0} I_{u_2}, \lim_{\rho\to 1} I_{u_2}\right) \neq \{\emptyset, 0\}. \quad (47)$$

Note that $\lim_{\rho\to 0} I_{u_1} = \lim_{\rho\to 1} I_{u_2} = 0$ can be easily obtained. Assuming $\rho \to \infty$, we have $P_{M,u_1} \to 0$ and $P_{F,u_1} \to 0$, and thus, $\lim_{\rho\to\infty} I_{u_1} \to 1$. Considering that I_{u_1} increases with the increase of ρ, we can obtain $\lim_{\rho\to 1} I_{u_1} \le 1$. Similarly, we can also have $\lim_{\rho\to 0} I_{u_2} \le 1$. At this point, (47) can be successfully proved. Finally, according to the principles of min-max (or max-min) based allocation described in [58–60], the crossover point of I_{u_1} and I_{u_2}, i.e., ρ_{opt}, is the optimal solution to (33).

Appendix C

Applying the allocation coefficient ρ to (25), we can explicitly show that (36) is a function of ρ, expressed as $\Gamma(\rho) = \mu_{u_1}I_{u_1} + \mu_{u_2}I_{u_2}$. First, let us first show that $\Gamma(\rho)$ is a concave function. To this purpose, we calculate the second derivative of $\Gamma(\rho)$, which is

$$\frac{d^2\,\Gamma(\rho)}{d\rho^2} = \frac{1}{2}\sum_k \mu_{u_k}\Bigg\{P''_{M,u_k}\log_2\mathcal{M}_k + P''_{F,u_k}\log_2\mathcal{F}_k + \frac{1}{\ln 2}\left(\frac{\left(P'_{M,u_k}\right)^2}{P_{M,u_k}\left(1-P_{M,u_k}\right)} - \frac{\left(P'_{M,u_k} - P'_{F,u_k}\right)^2}{\mathcal{W}_k}\right)$$

$$+\frac{1}{\ln 2}\left(\frac{\left(P'_{F,u_k}\right)^2}{P_{F,u_k}\left(1-P_{F,u_k}\right)}-\frac{\left(P'_{F,u_k}-P'_{M,u_k}\right)^2}{\mathcal{W}_k}\right)\Bigg\}, \quad (48)$$

where $\mathcal{W}_k = (1-P_{F,u_k}+P_{M,u_k})(1-P_{M,u_k}+P_{F,u_k})$. Specifically for user u_1, we have

$$P''_{M,u_1} = -\frac{1}{4}\sqrt{\frac{\mathcal{Q}}{8\pi}}\sum_{x_{u_1}^{(l-1)}\in\beta}\eta_{u_1,1}e^{-\frac{1}{2}\rho\mathcal{Q}\eta_{u_1,1}^2} \times\left(\frac{1}{\sqrt{\rho^3}}+\frac{1}{\sqrt{\rho}}\mathcal{Q}\eta_{u_1,1}^2\right)>0,$$

$$P''_{F,u_1} = \frac{1}{4}\sqrt{\frac{\mathcal{Q}}{8\pi}}\sum_{x_{u_1}^{(l-1)}\in\beta}\eta_{u_1,0}e^{-\frac{1}{2}\rho\mathcal{Q}\eta_{u_1,0}^2} \times\left(\frac{1}{\sqrt{\rho^3}}+\frac{1}{\sqrt{\rho}}\mathcal{Q}\eta_{u_1,0}^2\right)>0. \quad (49)$$

For user u_2, we also have

$$P''_{M,u_2} = -\frac{1}{4}\sqrt{\frac{\mathcal{Q}}{8\pi}}\sum_{x_{u_2}^{(l-1)}\in\beta}\eta_{u_2,1}e^{-\frac{1}{2}(1-\rho)\mathcal{Q}\eta_{u_2,1}^2} \times\left(\frac{1}{\sqrt{(1-\rho)^3}}+\mathcal{Q}\eta_{u_2,1}^2\sqrt{\frac{1}{1-\rho}}\right)>0$$

$$P''_{F,u_2} = \frac{1}{4}\sqrt{\frac{\mathcal{Q}}{8\pi}}\sum_{x_{u_2}^{(l-1)}\in\beta}\eta_{u_2,0}e^{-\frac{1}{2}(1-\rho)\mathcal{Q}\eta_{u_2,0}^2}, \times\left(\frac{1}{\sqrt{(1-\rho)^3}}+\mathcal{Q}\eta_{u_2,0}^2\sqrt{\frac{1}{1-\rho}}\right)>0. \quad (50)$$

Substituting the above results into (48) and considering $P_{M,u_k}+P_{F,u_k}<1$ as demonstrated in Appendix B, we can see that the first two terms on the right side of (48) are negative, whist the last two terms are positive. However, it is highly involved to directly determine the sign of $\frac{d^2\,\Gamma(\rho)}{d\rho^2}$. Therefore, we verify this by numerical results. As shown in Section IV (Numerical results, Fig. 6), when the assignment for the types of molecules is fixed, the objective function of (36) with respect to ρ is a concave function.

To go forward, we verify that there is a ρ, i.e., $\rho=\rho_{opt}$ such that $\frac{d\,\Gamma(\rho)}{d\rho}=0$, where

$$\frac{d\Gamma\left(\rho\right)}{\rho}=\sum_k \mu_k\frac{dI_{u_k}}{d\rho}. \quad (51)$$

Based on the previous analysis, it is obvious that $\frac{dI_{u_2}}{d\rho}<0<\frac{dI_{u_1}}{d\rho}$. Moreover, considering that $\frac{d\Gamma(\rho)}{\rho}$ is a continuous function over the entire domain, we can conclude that if

$$\mu_1\left(\lim_{\rho\to 0}\frac{dI_{u_1}}{d\rho},\lim_{\rho\to 1}\frac{dI_{u_1}}{d\rho}\right)\cap \mu_2\left(\left|\lim_{\rho\to 0}\frac{dI_{u_2}}{d\rho}\right|,\left|\lim_{\rho\to 1}\frac{dI_{u_2}}{d\rho}\right|\right)\neq\{\emptyset,0\}, \quad (52)$$

there is a $\rho=\rho_{opt}$ making $\frac{d\,\Gamma(\rho_{opt})}{d\rho_{opt}}=0$. Furthermore, for user u_1, we can obtain

$$\lim_{\rho\to 0}\frac{dI_{u_1}}{d\rho}=\frac{\mathcal{Q}}{(8\ln 2)\pi}\varepsilon^2,\quad \lim_{\rho\to 1}\frac{dI_{u_1}}{d\rho}=0, \quad (53)$$

while for user u_2, we can obtain

$$\lim_{\rho\to 0}\frac{dI_{u_2}}{d\rho}=0,\quad \lim_{\rho\to 1}\frac{dI_{u_2}}{d\rho}=-\frac{\mathcal{Q}}{(8\ln 2)\pi}\theta^2. \quad (54)$$

where

$$\varepsilon=\sum_{x_{u_1}^{(l-1)}\in\beta}\left(\eta_{u_1,1}+\eta_{u_1,0}\right),$$
$$\theta=\sum_{x_{u_2}^{(l-1)}\in\beta}\left(\eta_{u_2,1}+\eta_{u_2,0}\right). \quad (55)$$

At this point, we can conclude that in all the cases there is a $\rho=\rho_{opt}$ to make $\frac{d\,\Gamma(\rho_{opt})}{d\rho_{opt}}=0$ hold. Additionally, given $\frac{d^2\Gamma(\rho)}{(\rho)^2}<0$, we further conclude that ρ_{opt} is the optimal solution to (36).

REFERENCES

[1] Z. Ning *et al.*, "Partial computation offloading and adaptive task scheduling for 5G-enabled vehicular networks," *IEEE Trans. Mobile Comput.*, to appear.

[2] Z. Ning *et al.*, "Intelligent edge computing in internet of vehicles: A joint computation offloading and caching solution," *IEEE Trans. Intell. Transport. Syst.*, pp. 1–14, May 2020.

[3] V. Chamola, V. Hassija, V. Gupta, and M. Guizani, "A comprehensive review of the COVID-19 pandemic and the role of IoT, drones, AI, blockchain, and 5G in managing its impact," *IEEE Access*, vol. 8, pp. 90225–90265, 2020.

[4] A. Roy, F. H. Kumbhar, H. S. Dhillon, N. Saxena, S. Y. Shin, and S. Singh, "Efficient monitoring and contact tracing for COVID-19: A smart IoT-based framework," *IEEE Internet Things J. Mag.*, vol. 3, no. 3, pp. 17–23, Sept. 2020.

[5] F. Al-Turjman and B. Deebak, "Privacy-aware energy-efficient framework using the Internet of Medical Things for COVID-19," *IEEE Internet Things J. Mag.*, vol. 3, no. 3, pp. 64–68, Sept. 2020.

[6] Z. Ning *et al.*, "Mobile edge computing enabled 5G health monitoring for Internet of medical things: A decentralized game theoretic approach," *IEEE J. Sel. Areas Commun.*, to appear.

[7] I. F. Akyildiz, M. Pierobon, S. Balasubramaniam, and Y. Koucheryavy, "The Internet of bio-nano things," *IEEE Commun. Mag.*, vol. 53, no. 3, pp. 32–40, Mar. 2015.

[8] B. Atakan, O. B. Akan, and S. Balasubramaniam, "Body area nanonetworks with molecular communications in nanomedicine," *IEEE Commun. Mag.*, vol. 50, no. 1, pp. 28–34, Jan. 2012.

[9] M. Kuscu and O. B. Akan, "The Internet of molecular things based on FRET," *IEEE Internet Things J.*, vol. 3, no. 1, pp. 4–17, Feb. 2016.

[10] T. Nakano *et al.*, "Performance evaluation of leader-follower-based mobile molecular communication networks for target detection applications," *IEEE Trans. Commun.*, vol. 65, no. 2, pp. 663–676, Feb. 2017.

[11] Y. Chen, P. Kosmas, P. S. Anwar, and L. Huang, "A touch-communication framework for drug delivery based on a transient microbot system," *IEEE Trans. Nanobiosci.*, vol. 14, no. 4, pp. 397–408, June 2015.

[12] L. Felicetti, M. Femminella, and G. Reali, "A molecular communications system for live detection of hyperviscosity syndrome," *IEEE Trans. Nanobiosci.*, vol. 19, no. 3, pp. 410–421, July 2020.

[13] O. B. Akan, H. Ramezani, T. Khan, N. A. Abbasi, and M. Kuscu, "Fundamentals of molecular information and communication science," *Proc. IEEE*, vol. 105, no. 2, pp. 306–318, Feb. 2017.

[14] T. Nakano, Y. Okaie, S. Kobayashi, T. Hara, Y. Hiraoka, and T. Haraguchi, "Methods and applications of mobile molecular communication," *Proc. IEEE*, vol. 107, no. 7, pp. 1442–1456, July 2019.

[15] T. Nakano, S. Kobayashi, T. Suda, Y. Okaie, Y. Hiraoka, and T. Haraguchi, "Externally controllable molecular communication," *IEEE J. Sel. Areas Commun.*, vol. 32, no. 12, pp. 2417–2431, Dec. 2014.

[16] S. Ghavami, "Anomaly detection in molecular communications with applications to health monitoring networks," *IEEE Trans. Mol. Biol. Multi-Scale Commun.*, vol. 6, no. 1, pp. 50–59, July 2020.

[17] M. Khalid, O. Amin, S. Ahmed, B. Shihada, and M. Alouini, "Modeling of viral aerosol transmission and detection," *IEEE Trans. Commun.*, vol. 68, no. 8, pp. 4859–4873, Aug. 2020.

[18] M. Khalid, O. Amin, S. Ahmed, B. Shihada, and M. Alouini, "Communication through breath: Aerosol transmission," *IEEE Commun. Mag.*, vol. 57, no. 2, pp. 33–39, Feb. 2019.

[19] F. Gulec and B. Atakan, "A molecular communication perspective on airborne pathogen transmission and reception via droplets generated by coughing and sneezing," 2020. [Online]. Available: arXiv:2007.07598.

[20] F. Gulec and B. Atakan, "A droplet-based signal reconstruction approach to channel modeling in molecular communication," *IEEE Trans. Mol. Biol. Multi-Scale Commun.*, to appear.

[21] Y. Zamiri-Jafarian, S. Gazor, and H. Zamiri-Jafarian, "Molecular code division multiple access in nano communication systems," in *Proc. IEEE Wireless Commun. and Net. Conf.*, Doha, Qatar, Apr. 2016, pp. 1–6.

[22] L. Wang and A. W. Eckford, "Nonnegative code division multiple access techniques in molecular communication," in *Proc. 2017 15th Canadian Workshop on Inf. Theory (CWIT)*, Quebec City, Canada, July 2017, pp. 1–5.

[23] S. Korte, M. Damrath, M. Damrath, and P. A. Hoeher, "Multiple channel access techniques for diffusion-based molecular communications," in *Proc. Int. ITG Conf. Sys., Commun. and Coding (SCC)*, Hamburg, Germany, Feb. 2017, pp. 1-6.

[24] L. Shi, L.-L. Yang, and K.-C. Chen, "Molecular code-division multiple-access: Signaling, signal detection and performance," 2020. [Online]. https://www.researchgate.net/publication/339602272.

[25] Sasitharan Balasubramaniam *et al.*, "Development of artificial neuronal networks for molecular communication," *Nano Commun. Netw.*, vol. 2, no. 2–3, pp. 150–160, Sept. 2011.

[26] H. Tezcan, S. Oktug, and F. N. Kok, "Neural delay lines for TDMA based molecular communication in neural networks," in *Proc. IEEE Int. Conf. Commun. (ICC)*, Ottawa, Cananda, June 2012, pp. 6209–6213.

[27] M. J. Moore, Y. Okaie, and T. Nakano, "Diffusion-based multiple access by nano-transmitters to a micro-receiver," *IEEE Commun. Lett.*, vol. 18, no. 3, pp. 385–388, Mar. 2014.

[28] J. Suzuki, S. Balasubramaniam, and A. Prina-Mello, "Multi-objective TDMA optimization for neuron-based molecular communication," in *Proc. BODYNETS*, Oslo, Norway, Feb. 2012, pp. 40–47.

[29] R. Yu, M. S. Leeson, and M. D. Higgins, "Multiple-access scheme optimisation for artificial neuronal networks," in *Proc. Int. Symp. Commun. Syst., Net. Digital Sign (CSNDSP)*, Manchester, UK, July 2014, pp. 428–433.

[30] H. K. Rudsari, N. Mokari, M. R. Javan, E. A. Jorswieck, and M. Orooji, "Drug release management for dynamic TDMA-based molecular communication," *IEEE Trans. Mol. Biol. Multi-Scale Commun.*, vol. 5, no. 3, pp. 233–246, Dec. 2019.

[31] M. J. Moore and T. Nakano, "Multiplexing over molecular communication channels from nanomachines to a micro-scale sensor device," in *Proc. IEEE Global Commun. Conf. (GLOBECOM)*, Anaheim, USA, Dec. 2012, pp. 4302–4307.

[32] Y. Okaie, T. Nakano, M. Moore, and J.-Q. Liu, "Information transmission through a multiple access molecular communication channel," in *Proc. IEEE Int. Conf. Commun. (ICC)*, Budapest, Hungary, June 2013, pp. 4030–4034.

[33] L. Parcerisa and I. F. Akyildiz, "Molecular communication options for long range nanonetworks," *Computer Networks*, vol. 53, no. 16, pp. 2753–2766, Aug. 2009.

[34] O. U. Akgul and B. Canberk, "An interference-free and simultaneous molecular transmission model for multi-user nanonetworks," *Nano Commun. Netw.*, vol. 5, no. 4, pp. 83–96, Sept. 2014.

[35] N. Farsad, H. B. Yilmaz, C.-B. Chae, and A. Goldsmith, "Energy model for vesicle-based active transport molecular communication," in *Proc. IEEE Int. Conf. Commun. (ICC)*, Kuala Lumpur, Malaysia, May 2016, pp. 1–6.

[36] M. C. Gursoy, A. E. Pusane, and T. Tugcu, "Molecule-as-a-frame: A frame based communication approach for nanonetworks," *Nano Commun. Netw.*, no. 16, pp. 45–59, Jun. 2018.

[37] B. Atakan and O. B. Akan, "Single and multiple-access channel capacity in molecular nanonetworks," in *Proc. Int. Conf. Nano-Netw.*, Luzern, Switzerland, Oct. 2009, pp. 14–23.

[38] M. S. Kuran, H. B. Yilmaz, T. Tugcu, and I. F. Akyildiz, "Modulation techniques for communication via diffusion in nanonetworks," in *Proc. IEEE Int. Conf. Commun.(ICC)*, Kyoto, Japan, June 2011, pp. 1–5.

[39] N. R. Kim and C.-B. Chae, "Novel modulation techniques using isomers as messenger molecules for nano communication networks via diffusion," *IEEE J. Select. Areas Commun.*, vol. 31, no. 12, pp. 847–856, Dec. 2013.

[40] S. Giannoukos, A. Marshall, S. Taylor, and J. Smith, "Molecular communication over gas stream channels using portable mass spectrometry,", *J. Am. Soc. Mass Spectrom.*, vol. 28, no. 11, pp. 2371–2383, July 2017.

[41] D. T. McGuiness, S. Giannoukos, A. Marshall, and S. Taylor, "Experimental results on the open-air transmission of macro-molecular communication using membrane inlet mass spectrometry," *IEEE Commun. Lett.*, vol. 22, no. 12, pp. 2567–2570, Dec. 2018.

[42] M. Kuran, H. B. Yilmaz, T. Tugcu, and B. Ozerman, "Energy model for communication via diffusion in nanonetworks," *Nano Commun. Netw.*, vol. 1, no. 2, pp. 86–95, June 2010.

[43] C. Jiang, Y. Chen, and K. J. Ray Liu, "Nanoscale molecular communication networks: A game-theoretic perspective," *EURASIP J. Adv. Signal Process.*, vol. 2015, no. 1, p. 5, Jan. 2015.

[44] A. Ahmadzadeh, A. Noel, and R. Schober, "Analysis and design of multi-hop diffusion-based molecular communication networks," *IEEE Trans. Mol. Biol. Multi-Scale Commun.*, vol. 1, no. 2, pp. 144–157, June 2015.

[45] S. K. Tiwari, T. R. T. Reddy, P. K. Upadhyay, and D. B. Da Costa, "Joint optimization of molecular resource allocation and relay positioning in diffusive nanonetworks," *IEEE Access*, vol. 6, pp. 67681–67687, Nov. 2018.

[46] Y. Fang, A. Noel, N. Yang, A. W. Eckford, and R. A. Kennedy, "Symbol-by-symbol maximum likelihood detection for cooperative molecular communication," *IEEE Trans. Commun.*, vol. 67, no. 7, pp. 4885–4899, July 2019.

[47] A. Noel, K. C. Cheung, and R. Schober, "Using dimensional analysis to assess scalability and accuracy in molecular communication," in *Proc. IEEE Int. Conf. Commun. Workshops (ICC)*, Budapest, Hungary, Jun. 2013, pp. 818–823.

[48] I. Llatser, A. C.-Aparicio, M. Pierobon, and E. Alarcon, "Detection techniques for diffusion-based molecular communication," *IEEE J. Select. Areas Commun.*, vol. 31, no. 12, pp. 726–734, Dec. 2013.

[49] M. J. Moore and T. Nakano, "Oscillation and synchronization of molecular machines by the diffusion of inhibitory molecules," *IEEE Trans. Nanotechnol.*, vol. 12, no. 4, pp. 601–608, Jul. 2013.

[50] M. J. Moore, T. Nakano, A. Enomoto, and T. Suda, "Measuring distance from single spike feedback signals in molecular communication," *IEEE Trans. Signal Process.*, vol. 60, no. 7, pp. 3576-3587, Jul. 2012.

[51] H. ShahMohammadian, G. G. Messier, and S. Magierowski, "Blind synchronization in diffusion-based molecular communication channels," *IEEE Commun. Lett.*, vol. 17, no. 11, pp. 2156-2159, Nov. 2013.

[52] S. Abadal and I. F. Akyildiz, "Bio-inspired synchronization for nanocommunication networks," *in Proc. IEEE GLOBECOM*, Houston, US, ADec. 2011, pp. 1-5.

[53] D. Kilinc and O. Akan, "Receiver design for molecular communication," *IEEE J. Select. Areas Commun.*, vol. 31, no. 12, pp. 705–714, Dec. 2013.

[54] B. Tepekule, A. E. Pusane, H. B. Yilmaz, C.-B. Chae, and T. Tugcu, "ISI mitigation techniques in molecular communication," *IEEE Trans. Mol. Biol. Multi-Scale Commun.*, vol. 1, no. 2, pp. 202-216, June 2015.

[55] A. Noel, K. C. Cheung, and R. Schober, "Optimal receiver design for diffusive molecular communication with flow and additive noise," *IEEE Trans. NanoBiosci.*, vol. 13, no. 3, pp. 350–362, Sept. 2014.

[56] L. Shi and L.-L. Yang, "Error performance analysis of diffusive molecular communication systems with on-off keying modulation," *IEEE Trans. Mol. Biol. Multi-Scale Commun.*, vol. 3, no. 4, pp. 224–238, Dec. 2017.

[57] X. Chen, Y. Huang, L. Yang and M. Wen, "Generalized molecular-shift keying (GMoSK): Principles and performance analysis," *IEEE Trans. Mol. Biol. Multi-Scale Commun.*, to appear.

[58] J. Zhu, J. Wang, Y. Huang, S. He, X. You, and L. Yang, "On optimal power allocation for downlink non-orthogonal multiple access systems," *IEEE J. Select. Areas Commun.*, vol. 35, no. 12, pp. 2744–2757, Dec. 2017.

[59] J. Cui, Z. Ding, and P. Fan, "A novel power allocation scheme under outage constraints in NOMA systems," *IEEE Signal Process. Lett.*, vol. 23, no. 9, pp. 1226–1230, Sep. 2016.

[60] S. Timotheou and I. Krikidis, "Fairness for non-orthogonal multiple access in 5G systems," *IEEE Signal Process. Lett.*, vol. 22, no. 10, pp. 1647–1651, Oct. 2015.

Xuan Chen (S'19) received the B.S. degree from Wuhan University of Technology, Wuhan, China, in 2017. She is currently pursuing the Ph.D. degree with the South China University of Technology, Guangzhou, China. In August 2019, she was a visiting student for molecular communication in Yonsei University, Seoul, South Korea. Her main research interests include wireless and molecular communications.

She was the winner in data bakeoff competition (Molecular MIMO) at IEEE Communication Theory Workshop (CTW) 2019, Selfoss, Iceland.

Miaowen Wen (SM'18) received the Ph.D. degree from Peking University, Beijing, China, in 2014. From 2012 to 2013, he was a Visiting Student Research Collaborator with Princeton University, Princeton, NJ, USA. He is currently an Associate Professor with South China University of Technology, Guangzhou, China. He has published two books and more than 100 journal papers. His research interests include a variety of topics in the areas of wireless and molecular communications.

Dr. Wen was a recipient of the IEEE AsiaĺCPacific (AP) Outstanding Young Researcher Award in 2020, and four Best Paper Awards from the IEEE ITST'12, the IEEE ITSC'14, the IEEE ICNC'16, and the IEEE ICCT'19. He was the winner in data bakeoff competition (Molecular MIMO) at IEEE Communication Theory Workshop (CTW) 2019, Selfoss, Iceland. He served as a Guest Editor for the IEEE JOURNAL ON SELECTED AREAS IN COMMUNICATIONS and for the IEEE JOURNAL OF SELECTED TOPICS IN SIGNAL PROCESSING. Currently, he is serving as an Editor for the IEEE TRANSACTIONS ON COMMUNICATIONS, and the IEEE COMMUNICATIONS LETTERS, and a Guest Editor for the IEEE JOURNAL OF SELECTED TOPICS IN SIGNAL PROCESSING (Special Issue on Advanced Signal Processing for Local and Private 5G Networks).

Chan-Byoung Chae (F'20) received the Ph.D. degree in ECE from The University of Texas at Austin in 2008. He was a Research Engineer with the Telecommunications R&D Center, Samsung Electronics, Suwon, South Korea, from 2001 to 2005. He was with Harvard University, Cambridge, MA, USA, from 2008 to 2009, as a Post-Doctoral Research Fellow, and Bell Labs, Alcatel-Lucent, Murray Hill, NJ, USA from 2009 to 2011, as a Member of Technical Staff. He was a member of the Wireless Networking and Communications Group (WNCG), The University of Texas at Austin. He is currently an Underwood Distinguished Professor with the School of Integrated Technology, Yonsei University, South Korea.

He was a recipient/co-recipient of the Young Engineer Award from the IEEE VTS Daniel E. Noble Fellowship Award in 2008, the IEEE ComSoc AP Outstanding Young Researcher Award in 2012, the KICS Haedong Young Scholar Award in 2013, the IEEE Signal Processing Magazine Best Paper Award in 2013, the IEIE/IEEE Joint Award for Young IT Engineer of the Year in 2014, the IEEE INFOCOM Best Demo Award in 2015, the Yonam Research Award from LG Yonam Foundation in 2016, the Award of Excellence in Leadership of 100 Leading Core Technologies for Korea 2025 from the NAEK in 2017, the National Academy of Engineering of Korea (NAEK) in 2019, the IEEE DySPAN Best Demo Award in 2018, and the IEEE/KICS JOURNAL OF COMMUNICATIONS AND NETWORKS Best Paper Award in 2018. He has been serving as an Editor for IEEE COMMUNICATIONS MAGAZINE since 2016, IEEE TRANSACTIONS ON WIRELESS COMMUNICATIONS since 2012, IEEE TRANSACTIONS ON MOLECULAR, BIOLOGICAL, AND MULTI-SCALE COMMUNICATIONS since 2015, IEEE WIRELESS COMMUNICATIONS LETTERS since 2016, and IEEE/KICS JOURNAL OF COMMUNICATIONS AND NETWORKS since 2012. He is currently an Editorin-Chief of IEEE TRANSACTIONS ON MOLECULAR, BIOLOGICAL, AND MULTI-SCALE COMMUNICATIONS and a Senior Editor of IEEE WIRELESS COMMUNICATIONS LETTERS.

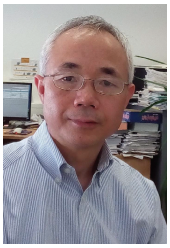

Lie-Liang Yang (F'16) received his BEng degree in communications engineering from Shanghai TieDao University, Shanghai, China in 1988, and his MEng and PhD degrees in communications and electronics from Northern (Beijing) Jiaotong University, Beijing, China in 1991 and 1997, respectively. From June 1997 to December 1997 he was a visiting scientist to the Institute of Radio Engineering and Electronics, Academy of Sciences of the Czech Republic. Since December 1997, he has been with the University of Southampton, United Kingdom, where he is the professor of Wireless Communications in the School of Electronics and Computer Science. He has research interest in wireless communications, wireless networks and signal processing for wireless communications, as well as molecular communications and nano-networks. He has published over 390 research papers in journals and conference proceedings, authored/co-authored three books and also published several book chapters. The details about his research publications can be found at https://www.ecs.soton.ac.uk/people/llyang. He is a fellow of both the IEEE and the IET, and was a distinguished lecturer of the IEEE VTS. He served as an associate editor to the IEEE Trans. on Vehicular Technology and Journal of Communications and Networks (JCN), and is currently an associate editor to the IEEE Access and a subject editor to the Electronics Letters.

Fei Ji (M'06) received the B.S. degree in applied electronic technologies from Northwestern Polytechnical University, Xiąan, China, and the M.S. degree in bioelectronics and Ph.D. degree in circuits and systems both from the South China University of Technology, Guangzhou, China, in 1992, 1995, and 1998, respectively. She was a Visiting Scholar with the University of Waterloo, Canada, from June 2009 to June 2010. She worked in the City University of Hong Kong as a Research Assistant from March 2001 to July 2002 and a Senior Research Associate from January 2005 to March 2005.

She is currently a Professor with the School of Electronic and Information Engineering, South China University of Technology. She was the Registration Chair and the Technical Program Committee (TPC) member of IEEE 2008 International Conference on Communication System. Her research focuses on wireless communication systems and networking.

Kostromitin Konstantin Igorevich graduated (Hons.) from the Municipal Secondary School, Chelaybinsk, Russia, and entered the Physical Department of Education, Chelaybinsk State University, Chelyabinsk, Russia, with specialization in physics. He received the bachelor's and master's degrees in physics with specialization in chair physics of condensed matter from Chelyabinsk State University, in 2008 and 2010, respectively, and the Ph.D. degree from Chelyabinsk State University, in 2013, with thesis entitled "Researching of Magnetocaloric Effect in Antiferromagnetics and Twins Moving in Heusler alloys" with specialization in physics of condensed matter in the Dissertation Council.